Talanta Open 9 (2024) 100278

Contents lists available at ScienceDirect

Talanta Open

journal homepage: www.sciencedirect.com/journal/talanta-open

A cutting-edge approach based on UHPLC-MS to simultaneously investigate oxysterols and cholesterol precursors in biological samples: Validation in Huntington's disease mouse model

Alice Passoni [a,*], Monica Favagrossa [b], Marta Valenza [c], Giulia Birolini [c,d], Alessia Lanno [a], Caterina Mariotti [e], Elena Cattaneo [c,d], Mario Salmona [b], Laura Colombo [b], Renzo Bagnati [a]

[a] Department of Environmental Health Sciences, Istituto di Ricerche Farmacologiche Mario Negri IRCCS, Milan, Italy
[b] Department of Molecular Biochemistry and Pharmacology, Istituto di Ricerche Farmacologiche Mario Negri IRCCS, Milan, Italy
[c] Department of Biosciences, University of Milan, Milan, Italy
[d] Istituto Nazionale di Genetica Molecolare "Romeo ed Enrica Invernizzi, Milan, Italy
[e] Unit of Medical Genetics, Fondazione IRCCS Istituto Neurologico Carlo Besta, Milan, Italy

ARTICLE INFO

Keywords:
Huntington's disease
Cholesterol metabolism
Liquid chromatography-mass spectrometry
Mouse plasma
Mouse brain

ABSTRACT

Brain is most cholesterol-rich organ in the body. Since cholesterol does not cross the blood brain barrier, its metabolism is provided *in situ* by astrocytes and neurons, and it is crucial for maintaining sterol levels and neuronal integrity and function. Recent studies have shown that the levels of cholesterol precursors and metabolites are lower in the brains of animal models of Huntington's disease (HD) while reduced levels of its catabolite are detected in the plasma of patients. In this study, we introduce a novel analytical method designed to fulfill the complex analytical requirements associated with cholesterol metabolites detection in neurodegenerative disorders. The method allows for the simultaneous quantification of a specific set of oxysterols along with cholesterol precursors in biological samples.

The proposed method uses an Ultra-High-Performance Liquid Chromatography-Mass Spectrometry (UHPLC-MS) system operating in multiple reaction monitoring (MRM). Since sterols can be found in biological matrices in either free form or esterified to various fatty acids, a three-step extraction procedure was devised, consisting of alkaline hydrolysis, liquid-liquid extraction and final concentration omitting the need for a solid-phase extraction (SPE) step.

The validated method achieved a detection limit of 10 ng/mL in plasma and 1 ng/mg in brain tissue, reaching a comparable sensitivity to previously published LC-MS and GC–MS methods. All target analytes were separated on a reverse-phase column employing a segmented gradient and a temperature ramp. This strategy enabled the elution and separation of all selected metabolites within a 30-minutes timeframe. This innovative approach was employed to quantify cholesterol metabolites in both plasma and brain samples from wild-type (WT) and R6/2 mice, a mouse model of HD. The results obtained from the sample analysis highlighted a significant reduction in desmosterol levels in the R6/2 brain at 12 weeks.

In conclusion, the proposed method paves the way for further development of high-sensitive and reproducible protocols to comprehensively investigate simultaneous alterations in both cholesterol biosynthesis and catabolism in HD samples.

1. Introduction

Chol (Chol), the most abundant member of sterols, is distributed in all tissues, serving as a fundamental component of all mammalian cell membranes and acting as the precursor to other important steroids, such as hormones and bile acids [1]. Although the brain represents only 2.1 % of the total body weight it contains 25 % of the total Chol present in the human body [2], mainly in non-esterified form (>99.5 %). In the brain, Chol originating during development serves as the main constituent of myelin. Additionally, newly synthesized Chol plays a pivotal role in

* Corresponding author.
E-mail address: alice.passoni@marionegri.it (A. Passoni).

https://doi.org/10.1016/j.talo.2023.100278
Received 25 September 2023; Received in revised form 25 November 2023; Accepted 5 December 2023
Available online 6 December 2023

neuronal function and synaptic communication [3]. It is widely distributed within specific regions of cell membranes called lipid rafts, which are essential for initiating, spreading, and sustaining signal transmission [4]. In the adult brain, Chol homeostasis is preserved through local production, predominantly from astrocytes, since circulating Chol cannot cross the blood-brain barrier (BBB). Consequently, over 95 % of brain Chol is produced *in situ* by *de novo* synthesis [5]. Importantly, any modifications in Chol production during brain development or in adulthood can affect neuronal maturation, recycling, synaptic vesicle fusion, and neurotransmitter receptor function. The structural significance of Chol is underscored by its considerably lower turnover rate in the brain, which is much slower (250–300 times) compared to the periphery [2].

Dysregulation or breakdown of brain cholesterol synthesis has been implicated in various disorders, including Huntington's disease (HD), which is an inherited neurodegenerative disorder resulting from abnormal cytosine-adenosine-guanine (CAG) repeat expansion in the human *IT15* gene's first exon [3]. This leads to the translation of an elongated polyQ tract ($Q > 40$) in the Huntingtin (HTT) protein, that cause symptoms and the manifestation of clinical symptoms such as cognitive decline, psychiatric disturbances, and choreiform movements [6,7,8]. Numerous molecular and cellular dysfunctions have been identified in HD cell lines, animal models, and human postmortem tissues, highlighting changes in brain cholesterol biosynthesis. In various HD animal models, Chol precursors such as lanosterol, lathosterol, and desmosterol, along with the activity of the 3-hydroxy-3-methylglutaryl-coenzyme A reductase (HMGCR), exhibit downregulation in the presymptomatic stage of the disease, leading to significantly lower Chol levels at later stages [9,10,11]. Lanosterol, a pivotal intermediate in Chol biosynthesis, can be metabolized via two distinct pathways: the Bloch pathway and the Kandutsch-Russel pathway, resulting in the synthesis of desmosterol/zymosterol and 7-dehydrocholesterol/lathosterol, respectively. Cholesterol formation is followed by its catabolism, generating several oxysterols, some of which are important neurosteroids. Within the brain, excessive cholesterol is catabolized by the enzyme 24-hydroxylase (CYP46A1), which regulates the conversion of Chol in 24S-hydroxycholesterol (24S-OHC), a molecule capable of crossing the BBB. Consequently, 24S-OHC emerges as a promising indicator of the reduced brain Chol metabolism during neurodegeneration, as reported in the literature [12,13]. Given these bases, the development of analytical methodologies enabling precise and simultaneous quantification of Chol precursors and metabolites within the brain becomes imperative.

The GC–MS method has long been the conventional approach to analyze oxysterols. Over the years, GC–MS remained the most reliable method to the extent that is often regarded as the "gold standard" for oxysterol analysis [14]. However, since the method requires a derivatization reaction that is applicable only to conjugated oxysterols after prior hydrolysis, the GC–MS method is known for its complex sample preparation. In 1995 Diczfalusy established the reference method for this type of analysis using GC–MS [15]. This method involved of alkaline hydrolysis followed by a liquid-liquid extraction, solid-phase extraction (SPE) purification and final derivatization using trimethylsilyl ethers.

While the current literature has documented several GC–MS methods for monitoring the Chol synthesis pathway [11,15–17], there has been a notable increase in the number of LC-MS methods since the 2000s [14, 18,19]. Interestingly, the derivatization and SPE steps, which are essential for GC–MS analysis, are also widely employed in LC-MS methods to enhance sensitivity [19].

Therefore, this study aims to introduce a state-of-the-art LC-MS approach capable of quantifying both oxysterols and cholesterol precursors in both plasma and brain samples within a single analytical run. The paper provides a comprehensive account of the sample preparation procedures, including the hydrolysis reaction, while highlighting the potential for optimization to simplify the process without compromising sensitivity. Furthermore, the proposed method was applied to characterize the brain sterol metabolism of R6/2 mice, an HD mouse model. These analyses revealed a significant decrease in desmosterol levels in the striatum of 12-week-old R6/2 mice when compared to their WT littermates.

2. Materials and methods

2.1. Standards and chemicals

LC-MS grade methanol and formic acid were from Carlo Erba, Milan, Italy. LC-MS grade deionized water was obtained from a Milli-Ro 60 Water System, Millipore, Milford, MA, USA. The standards 7-alphahydroxycholesterol, 24(*S*)-hydroxycholesterol, 25-hydroxycholesterol and 25(*S*)−27-hydroxycholesterol were purchased from VINCI-BIOCHEM Srl; 24-dehydrohydrocholesterol, 7-dehydrocholesterol, and lanosterol were purchased from CABRU S.A.S. The internal standards used for hydroxysteroid analysis were: 24(R/S)-hydroxycholesterol-D7 (SPECTRA 2000 Srl), 25-hydroxycholesterol-D6 (VINCI-BIOCHEM Srl), desmosterol-D6 (CABRU SAS) and lathosterol-D7 (Merck et al.). Cholesterol-D6 (Sigma-Aldrich) was used as the internal standard for cholesterol analysis. All standards were dissolved in ethanol (Carlo Erba) and stored at −20° as 1 mg/mL solutions.

Butylhydroxytoluene (BHT) was purchased from Acros Organics, potassium hydroxide from Merck Life Science S.r.l., ethanol and dichloromethane from Carlo Erba, and Phosphate Buffer Saline (PBS) from Fisher Scientific.

2.2. Animals

Procedures involving animals and their care were conducted in conformity with the institutional guidelines at the Istituto di Ricerche Farmacologiche Mario Negri IRCCS in compliance with national (D.lgs 26/2014; Authorization n. 19/2008-A issued March 6, 2008, by Ministry of Health) and international laws and policies (EEC et al. 2010/63/UE; the NIH Guide for the Care and Use of Laboratory Animals, 2011 edition). They were reviewed and approved by the Mario Negri Institute Animal Care and Use Committee, which includes ad hoc members for ethical issues, and by the Italian Ministry of Health (616–2018-PR and 786/2021-PR). Animal facilities meet international standards and are regularly checked by a certified veterinarian responsible for health monitoring, animal welfare supervision, experimental protocols, and review of procedures.

We used an R6/2 colony of mice generated to overexpress the first exon of the human mutant huntingtin gene with approximately 160 CAG repeats [20]. The animals had a 12 h h/night/day cycle with free water and food *ad libitum access*. Our R6/2 colony is maintained through crossing heterozygous R6/2 males and commercial wild-type females (B6CBAF1/J, purchased from Charles River). The R6/2 line was genotyped by polymerase chain reaction (PCR) on DNA from ear samples at weaning [20] . The experiments were conducted on 12 weeks old R6/2 mice and their littermates. At sacrifice, plasma and the striatum area were collected and stored at −80 °C until the analysis.

2.3. Sample preparation for Chol metabolites determination

The extraction method involved the addition of Internal Standards (IS) at the following concentrations: cholesterol precursors (desmosterol-D6 and lathosterol-D7) 100 ng/mg in brain tissues and 1 μg/mL in plasma and cholesterol metabolites (24-hydroxycholesterol-D7 and 25-hydroxycholesterol-D6) 10 ng/mg in tissues and 100 ng/mL in plasma.

- Plasma: 250 μL aliquots of plasma were spiked with IS. Samples were deproteinized in 2 mL tubes using a slow protein precipitation method using ethanol (EtOH) (containing 100 μg/mL BHT) in three separate aliquots of 500 μL each. After each addition, samples were stored at 4 °C for 15 min and, after the last addition, centrifuged at

13,200 rpm for 15 min. The main advantage of slow protein precipitation is the increase of the signal-to-noise ratio of the analytes without the necessity of an additional solid-phase extraction step. After deproteinization, the supernatants were recovered and hydrolyzed by adding 175 μL of 1 M KOH in water. The reaction was optimized for KOH concentration, time, and incubation temperature and was finally carried out at 37 °C for 1 h. After hydrolysis, 500 μL of water and 2 mL of dichloromethane (DCM) were added to samples for liquid-liquid extraction. Samples were mechanically mixed, sonicated for 30 min, and centrifuged for 15 min at 2400 rcf at room temperature. The extraction was repeated twice, and at each step, the organic phase was recovered and gently dried under nitrogen flow. The extracts were re-suspended in 40 μL EtOH for analysis.

- Brain tissues: 100 mg of tissues were homogenated in a 1:10 ratio with a PBS solution after adding the IS. Tissue homogenization was carried out with the Precellys system, using 2 mL screw-cap tubes containing 0.5 g of ceramic beads (zirconium oxide) with a diameter of 1.4 mm. The homogenizer can develop high energy and fully homogenates tissues through a three-dimensional rotation movement, which increases its speed from 4000 to 6800 rpm in two 45-second cycles separated by a 1-minute break. 200 μL of the homogenates were transferred to 1.5 mL tubes and extracted with 800 μL of EtOH containing 100 μg/mL BHT. Samples were vortexed and centrifuged at 13,200 rpm at 4 °C for 15 min. The supernatant (1 mL) was recovered and hydrolyzed by adding 125 μL of 1 M KOH in water. The reaction was conducted under controlled temperature conditions (40 °C) for 1 h. The hydrolyzed samples were added with 500 μL of water and 2 mL of DCM for the liquid-liquid extraction. Samples were mechanically mixed, sonicated for 30 min, and centrifuged for 15 min at 2400 rpm at room temperature. The extraction was repeated twice, and at each step, the organic phase was recovered and gently dried under nitrogen flow. The extracts were suspended in 100 μL EtOH for analysis.

2.4. Sample preparation for Chol determination

5 μL of plasma were spiked with cholesterol-D6 as IS at the final concentration of 1 mg/mL. Samples were deproteinized with 115 μL of EtOH containing 100 μg/mL BHT. They were vortex and centrifuged at 13,200 rpm at 4 °C for 15 min. 5 μL of the supernatants were diluted with 45 μL of ethanol and analyzed for the determination of free chol. The remaining supernatants were recovered and hydrolyzed by adding 20 μL of 1 M KOH in water. The reaction was carried out at 40 °C for 1 h. The hydrolyzed samples were added with 500 μL of water and 500 μL of DCM for the liquid-liquid extraction. Samples were mechanically mixed, sonicated for 30 min, and centrifuged for 15 min at 2400 rpm at room temperature. The extraction was repeated twice, and at each step, the organic phase was recovered and gently dried under nitrogen flow. The extracts were suspended in 1250 μL of EtOH to determine total Chol.

2.5. Instrumental analysis of Chol metabolites and precursors

The Chol metabolites and precursors were analyzed on a triple quadrupole operating in multiple reaction monitoring (MRM) mode interfaced to an ultra-high-performance liquid chromatography system (LCMS8060, Shimadzu). The mass spectrometer was equipped with an electrospray ionization (ESI) source operating in positive ions. A Shimpack XR-ODS III column (200 × 2.1 mm, 3 um) was used for the chromatographic separation of all substances. Metabolites and Chol-precursors were determined in a single chromatographic run, using a segmented gradient, slower in the first phase to efficiently separate the oxysterols isomers and faster in the second phase to guarantee an efficient elution of Chol precursors within 30 min. The chromatographic gradient was integrated with a temperature ramp to facilitate the elution of precursors in the second phase and to improve the peak shape. A flow rate of 0.30 mL/min was used. Table 1. resumes the chromatographic and temperature conditions.

Table 1
Scheme of temperature and solvent gradients of the developed UHPLC-MRM method.

Time	Phase B % (HCOOH 0.1 % in methanol) / Phase A % (HCOOH 0.1 % in water)	Column Temperature (°C)
0 min	84/16	40 °C
11 min	86/14	
14.5 min		40 °C
20 min	98/2	65 °C
31 min		65 °C
35 min		40 °C
42 min	98/2	
43 min	84/16	40 °C

Table 2 resumes the monitored transitions included in the MRM method, together with the corresponding optimized collision energies (CE).

2.6. Instrumental analysis of Chol

Chol levels were determined using a 1260 Series HPLC system (Agilent Technologies, USA) interfaced with an API 5500 triple quadrupole mass spectrometer (Sciex). The mass spectrometer was equipped with an atmospheric pressure chemical ionization (APCI) source operating in positive ion and MRM modes to measure the product ions obtained in a collision cell from the protonated $[M - H_2O]^+$ ions (Chol) or $[M - 2H_2O]^+$ (Chol-D6) of the analytes. The transitions identified during the optimization of the method were *m/z* 375.3–152.1 (quantification transition) and *m/z* 375.3–167.1 (qualification transition) for Chol-D6 (IS); *m/z* 397.3–147.1 (quantification transition) and *m/z* 397.3–161.1 (qualification transition) for Chol. The ion source settings were as follows: nebulized current (NC) 3; curtain gas (CUR) 30; collision gas (CAD) 7; source temperature 400 °C; ion source gas 1 (GS1) 60 and gas 2 (GS2) 30. Chol-D6 and Chol were separated on a Gemini C18 column (50 × 2 mm; 5 μm particle size) using an isocratic gradient in methanol at 35 °C.

Table 2
Selected MRM transitions and related Collision Energies (CE).

Analyte	Quantifier	CE	Qualifier	CE
7α-dihydroxycholesterol [7αHC]	383.5 → 159.3	27	383.5 → 105.1	45
24S-hydroxycholesterol [24S-OHC]	367.3 → 159.1	28	363.3 → 133.1	25
24-hydroxycholesterol-D_7 [24-OHC-D_7]	374.1 → 159.1	23	374.1 → 147.1	25
Lathosterol-D_7	376.3 → 161.1	24	376.3 → 105.1	45
25-hydroxycholesterol [25-OHC]	367.1 → 147.1	25	367.1 → 159.2	25
25-hydroxycholesterol-D_6 [25-OHC-D_6]	373.3 → 147.1	24	373.3 → 161.1	23
27-hydroxycholesterol [27-OHC]	385.2 → 161.1	21	385.2 → 135.1	24
Desmosterol [Desm]	367.2 → 147.1	24	367.2 → 95.1	30
Desmosterol-D_6 [Desm-D_6]	373.2 → 147.1	24	373.2 → 161.1	23
Lanosterol [Lan]	409.2 → 95.1	35	409.2 → 109.2	25
22-hydroxycholesterol [22-OHC]	367.3 → 159.3	25	367.3 → 91.2	54
7-dehydrocholesterol [7-dehydrochol]	367.2 → 159.1	21	367.2 → 95.3	34

2.7. Validation scheme for Chol metabolites

The LC-MS method was validated to ensure that the precision/accuracy of each analytical session was within 15 % of variation, expressed as CV %.

Since Chol metabolites are endobiotic compounds, the quantitation method was validated following the scheme reported in Table 3. PBS buffer was used as a surrogate matrix to simulate the extraction and hydrolysis step during the preparation of calibrants. In contrast, deuterated analytes were used as surrogate analytes to evaluate the influence of the matrix on recovery efficiency.

2.8. Statistical analysis

Prism 8 (GraphPad Software) was used to perform statistical analyses. G-power software was used to pre-determine group allocation, data collection and all related analyses. For animal studies, mice were assigned randomly, and sex was balanced in the various experimental groups; animals from the same litter were divided into different experimental groups; blinding of the investigator was applied to *in vivo* procedures and all data collection. Grubbs' test was applied to identify outliers. For each data set to be compared, we determined whether data were normally distributed or not to select parametric or not parametric statistical tests. The specific statistical test used is indicated in the legend of all results figures.

3. Results and discussion

3.1. Hydrolysis reaction setup

To optimize the hydrolysis reaction required for quantifying the Chol metabolites in their total form (ester bound plus free), we tested different experimental conditions, using plasma and plasma spiked with known concentrations of deuterated standards, starting from the more common conditions found in the literature.

Initially, we examined two different concentrations of KOH (10 M and 1 M) across three different temperatures (100 °C, 50 °C and 37 °C). These chosen concentrations are frequently encountered in the literature, with one of them being employed in a method previously established in our Institute, as detailed by Villani et al. [21]. Table 4 summarizes the hydrolysis conditions tested. For each experimental group, a biological triplicate was analyzed.

Analysis of samples hydrolyzed with 10 M KOH showed no signals corresponding to oxysterols. Conversely, for of samples incubated with 1 M KOH, distinct quantifiable signals were observed, with no significant discrepancies across different temperatures (One-way ANOVA test). This result highlighted that an elevated KOH triggers the degradation of analytes or significant ion suppression, leading to inadequate sensitivity for oxysterols detection. The outcomes are presented in Fig. 1 and Table 5 show casing the effects of varying KOH concentrations.

After identifying the best KOH concentration, the effect of the different temperatures was evaluated. Although there was no significant difference between the calculated concentrations using a different temperature of incubation, the evaluation of the analytes' peak areas showed clear differences. Peak areas for oxysterols and relative IS doubled after incubation at 37 °C. Fig. 2 and Table 6 showed the peak areas of the oxysterols and the relative IS under different experimental conditions.

Table 3
Validation scheme for Chol metabolites method.

Method validation: Chol metabolites	
Matrix Effects and Extraction Recovery	Surrogate analyte
Calibration Curve, Linearity	Surrogate matrix
Accuracy	Surrogate matrix
Precision	Surrogate matrix

Table 4
Hydrolysis conditions tested for method setup.

Experimental group	KOH Concentration (M)	Temperature (°C)
1	10 M	100 °C
2	10 M	50 °C
3	10 M	37 °C
4	1 M	100 °C
5	1 M	50 °C
6	1 M	37 °C

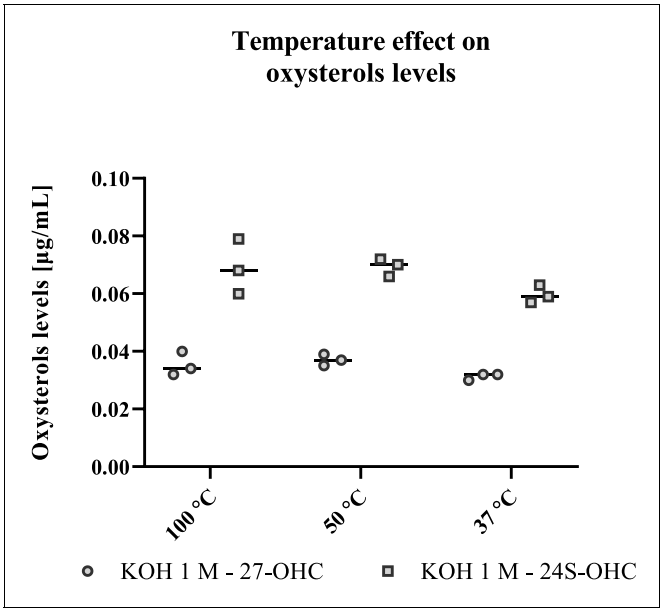

Fig. 1. Scatter dot plot representing 24S-OHC and 27-OHC levels in plasma samples after hydrolysis (each dot: technical replicate, line: mean; $N = 3$/experimental group).

Table 5
24S-OHC and 27-OHC levels in plasma samples after hydrolysis with KOH 1 M ($N = 3$/experimental group).

Analyte		KOH 1 M		
		100 °C	50 °C	37 °C
24S-OHC	µg mL	0.074	0.068	0.06
	SD	0.01	0.003	0.004
	CV	11 %	4 %	7 %
27-OHC	µg mL	0.035	0.037	0.031
	SD	0.004	0.002	0.001
	CV	12 %	5 %	4 %

Following the determination of the optimal conditions for KOH concentration and incubation temperature, subsequent experiments were conducted to identify the best reaction time. In literature, hydrolysis is often carried out for 1 h, but shorter or longer times are used in other studies [15,22–25]. In this regard, we set up an experiment encompassing four different incubation times, starting from 15 min and extending to 120 min (Table 7).

The results obtained from the measurement of Chol and Chol-D6 are reported in the following figure (Fig. 3), as an example of the effects of the incubation time on the analytes' peak area. It is evident that the areas of analytes and IS decreased if the sample was incubated for 2 h h, while up to an h, the areas were comparable. Consequently, we confirmed 1 h as the best incubation time to attain complete analyte hydrolysis, ensuring optimal signal-to-noise ratios.

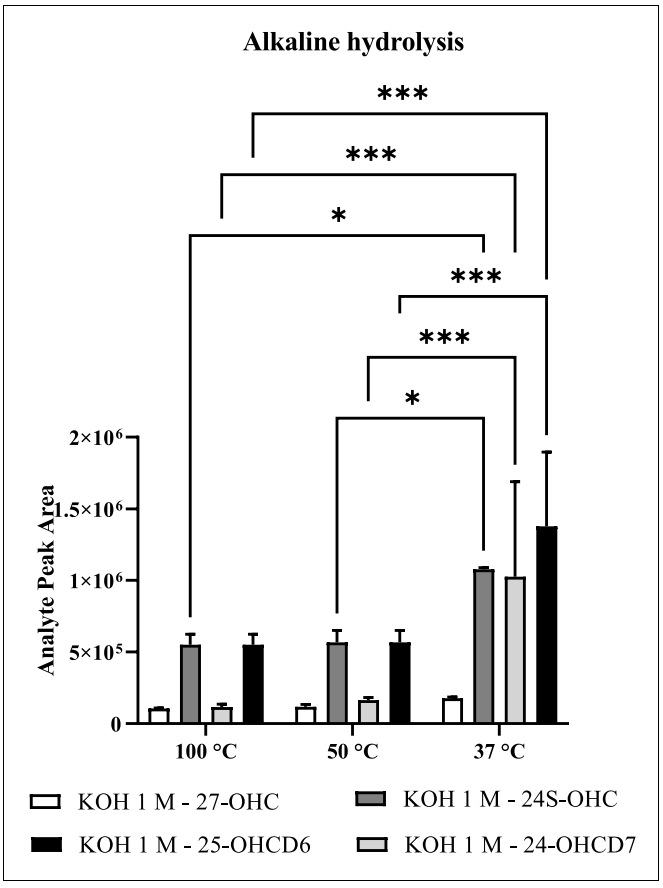

Fig. 2. Bar Chart representing oxysterols and relative IS peak areas under different hydrolysis conditions, error bars represent standard errors. Statistics: One-way ANOVA, Tukey's test (p-value: *<0.05, **<0.01, ***<0.005).

Table 6
Oxysterols and relative IS peak areas under different hydrolysis conditions.

Analyte		100 °C	50 °C	37 °C
24-OHC-D7	Mean Peak Area	1.16E+05	1.64E+05	1.03E+06
	SD	1.98E+04	1.96E+04	6.64E+05
	CV (%)	17 %	12 %	65 %
24-OHC	Mean Peak Area	5.51E+05	5.68E+05	1.08E+06
	SD	7.32E+04	8.30E+04	1.11E+04
	CV (%)	13 %	15 %	1 %
25-OHC-D6	Mean Peak Area	5.51E+05	5.68E+05	1.38E+06
	SD	7.32E+04	8.30E+04	5.19E+05
	CV (%)	13 %	15 %	38 %
27OHC	Mean Peak Area	1.06E+05	1.17E+05	1.78E+05
	SD	3.44E+03	1.79E+04	7.29E+03
	CV (%)	3 %	15 %	4 %

Table 7
Experimental conditions tested for the identification of the best time of incubation.

Experimental group	[KOH]	Temperature	Time of incubation
1	1 M	37 °C	15 min
2			30 min
3			60 min
4			120 min

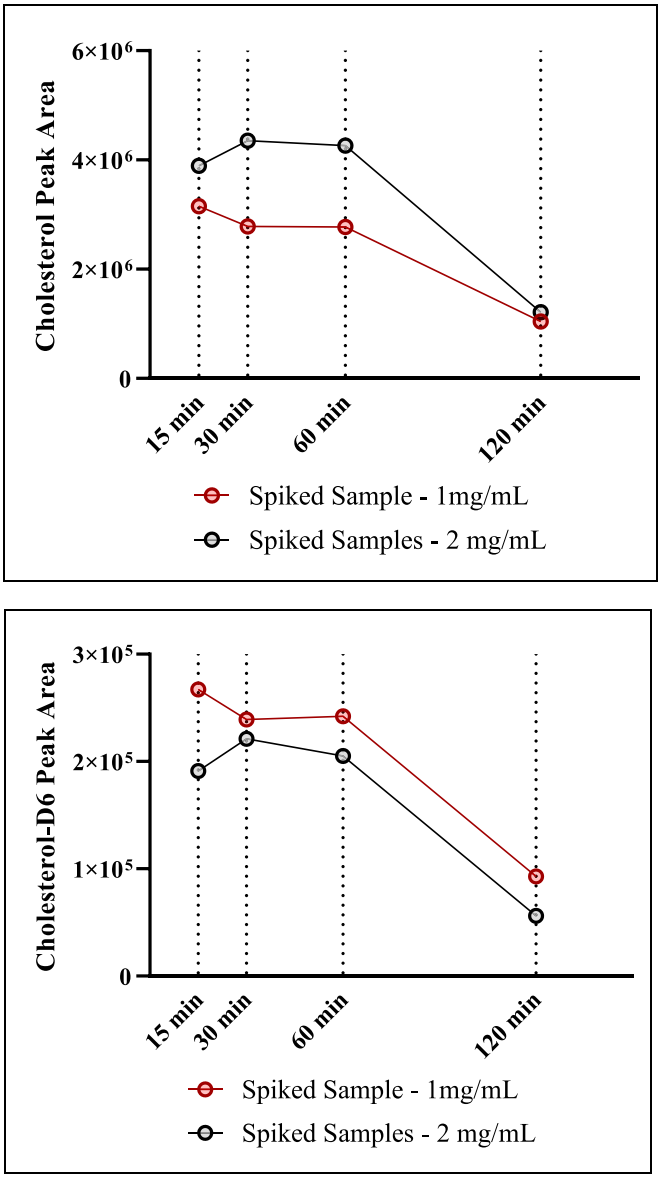

Fig. 3. Results of the optimization of the incubation time with KOH 1 M (samples spiked with two different concentrations of Chol (1 mg/mL and 2 mg/mL) and fixed Chol-D6 used as IS (1 mg/mL)).

3.2. Development and validation of the LC-MS methods

Validation data are reported in detail in the Supplementary Results.

3.3. Validation of the optimized hydrolysis reaction with a commercial kit

To evaluate the efficacy of the optimized hydrolysis reaction, we compared the results of measuring free and total Chol in plasma samples using both our analytical method and the Amplex™ Red Cholesterol Assay Kit (Thermo Scientific). The Amplex™ Red Cholesterol Assay Kit offers a highly sensitive, rapid, and straightforward fluorometric method to detect exceedingly low Chol concentrations, employing a fluorescence microplate reader. Here we employed independent plasma samples and examined the correlation between quantified Chol levels ($N = 15$). Each plasma sample was divided into two aliquots: one destined for our in-house developed extraction method followed by LC-MS analysis, and the other for the commercial kit analysis followed by fluorometric detection.

Table 8 resumes the results obtained, highlighting a high grade

Table 8
Quantified Chol levels using a commercial kit and in-house developed and validated method based on LC-MS.

Chol measured Level (mg/mL)	Commercial Kit	LC-MS
Sample 1	1.51	1.79
Sample 2	1.16	1.47
Sample 3	0.99	0.96
Sample 4	1.33	1.64
Sample 5	1.35	1.74
Sample 6	1.14	1.66
Sample 7	1.18	1.29
Sample 8	1.34	1.69
Sample 9	1.21	1.14
Sample 10	1.31	1.28
Sample 11	1.48	1.37
Sample 12	1.53	2.11
Sample 13	1.15	1.34
Sample 14	1.37	1.78
Sample 15	1.38	1.52

according to the results obtained.

The statistical analysis (Spearman correlation) confirmed the existence of a significant correlation between the results obtained using the two methods (Fig. 4). This validation of our extraction and hydrolysis method gave us confidence in the method's sound performance. In order to assess the robustness of the analytical method, we set up a brief method validation, taking into account the limitations of the method validation for endobiotic compounds, such as Chol metabolites.

3.4. Chol metabolites analysis in brain and plasma from R6/2 mice

In this study, we aimed to identify and analyze brain Chol metabolism *in vivo* by evaluating the concentration of desmosterol and 7-dehydrocholesterol, both Chol precursors, alongside the concentration of 24S-OHC, which serves as an indicator of Chol metabolism rate within the brain. To assess the setup method, we analyzed striatum tissues and plasma samples obtained from 12-week-old R6/2 mice at the symptomatic stage of the disease, in comparison to their WT. littermates. We observed that the desmosterol levels in the striatum of R6/2 mice were significantly lower than those in the WT mice. This indicates that the Bloch pathway, predominantly used by astrocytes, was notably impaired in the symptomatic stage of R6/2 animals. However, there were no differences in the 7-dehydrocholesterol levels between the two experimental groups in striatum tissues (Fig. 5).

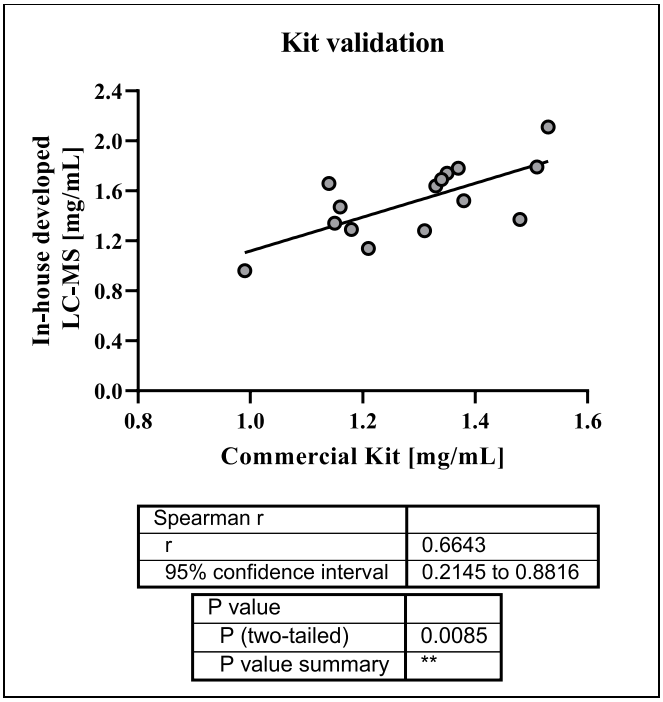

Fig. 4. Comparison between the Chol analysis using a commercial kit and in-house developed hydrolysis method. Statistics: Spearman correlation (p-value: **<0.01).

Furthermore, we also evaluated the steady-state Chol metabolism in the brain, by measuring the levels of 24S-OHC. We observed a significant reduction in its concentration in R6/2 mouse brain when compared to WT mice. This observation implies that Chol catabolism is also affected in the brain of R6/2 mice at the symptomatic stage. Additionally, we examined the plasmatic 24S-OHC levels. However, we found no difference in the amount of 24S-OHC in plasma samples between R6/2 and WT animals. This discrepancy might be attributed to the influence of peripheral Chol metabolism in mouse models, which differs from that in humans

Our results demonstrate the efficacy of the developed analytical method in simultaneously uncovering defects in the Bloch pathway and Chol catabolism in the brain of R6/2 mice at the symptomatic stage of the disease. These findings may contribute to a better understanding of Chol metabolism in neurodegenerative diseases and offer implications for the potential development of therapeutic interventions.

4. Conclusions

A reproducible and reliable LC-MS method has been successfully validated for the precise quantification of Chol precursors and metabolites in both mouse brain tissues and plasma samples. Our optimization efforts encompassed investigating KOH concentration, incubation temperature, and reaction duration for the hydrolysis step. Ultimately, we determined that the optimal reaction condition involve incubating samples for at 37 °C with 1 M KOH for 1 h, as this results in complete analyte hydrolysis and optimal signal-to-noise ratios. Additionally, the robustness of our LC-MS method is underscored by a comparative analysis with a commercial cholesterol kit.

Moreover, we established the linearity of all analytes over a wide concentration range demonstrating satisfactory precision and accuracy in both plasma and brain tissues. This validated method was used to investigate the disruption in Chol metabolism in the R6/2 mouse model, revealing a decrease in both Chol synthesis and catabolism in the brain of symptomatic R6/2 mice compared to their WT littermates. Furthermore, this method applicability extends to human plasma, where all 24S-OHC is of cerebral origin [26]. Its potential use in human plasma could enhance our comprehension of brain Chol metabolism in individuals with HD, allowing exploration of the role of these alterations as potential biomarkers not only for HD but also for other neurodegenerative disorders involving disruptions in brain Chol metabolism.

CRediT authorship contribution statement

Alice Passoni: Conceptualization, Formal analysis, Writing – review & editing. **Monica Favagrossa:** Conceptualization, Formal analysis, Writing – review & editing. **Marta Valenza:** Writing – review & editing, Funding acquisition. **Giulia Birolini:** Writing – review & editing, Funding acquisition. **Alessia Lanno:** Writing – review & editing, Funding acquisition. **Caterina Mariotti:** Funding acquisition. **Elena Cattaneo:** Funding acquisition. **Mario Salmona:** Writing – review & editing, Funding acquisition. **Laura Colombo:** Conceptualization, Formal analysis. **Renzo Bagnati:** Conceptualization, Formal analysis.

Declaration of Competing Interest

The authors declare that they have no known competing financial interests or personal relationships that could have appeared to influence the work reported in this paper.

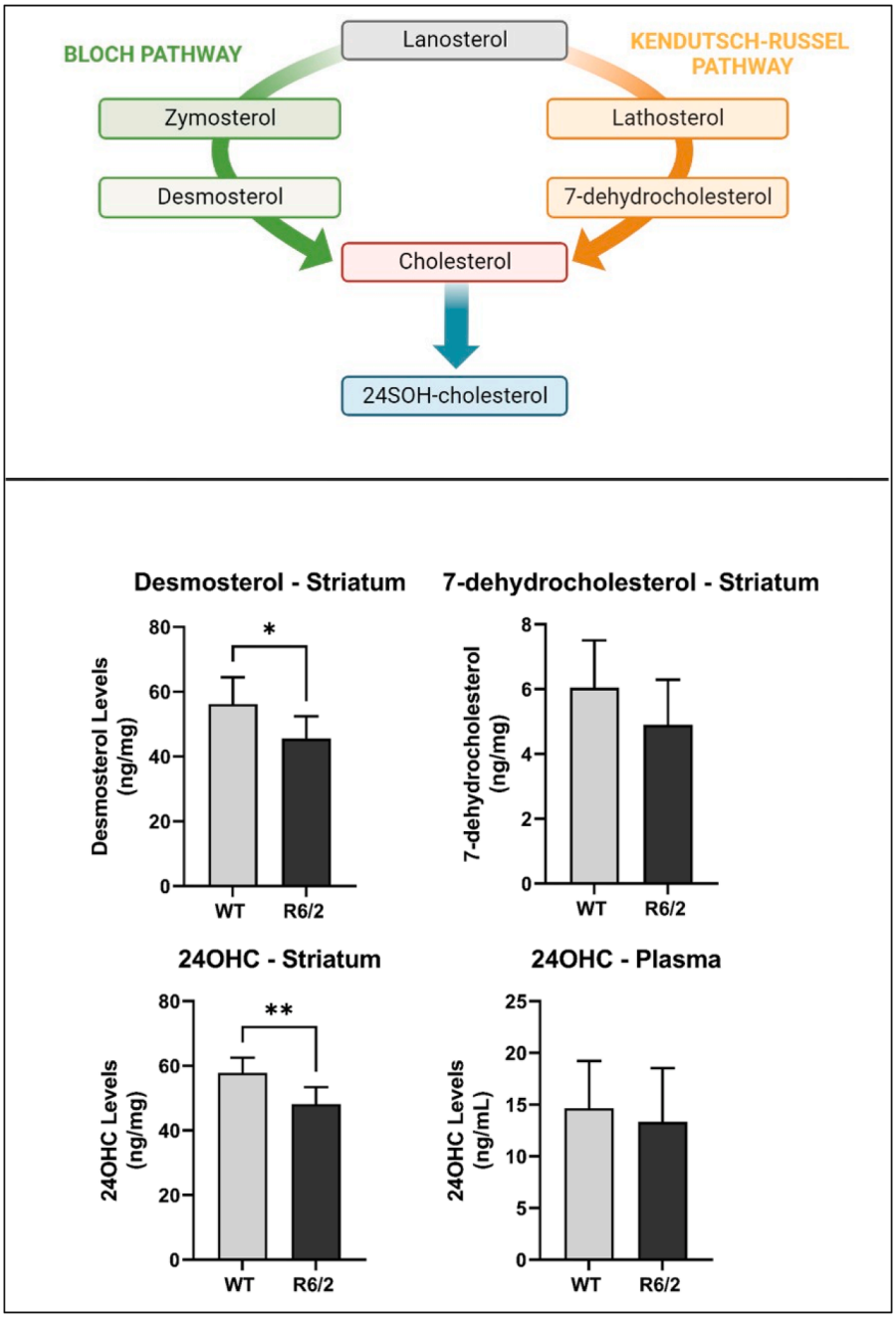

Fig. 5. Upper panel: Block scheme of Chol metabolic pathway; Lower panel: Desmosterol, 7-dehydrocholesterol and 24S-OHC levels in striatum area in WT, R6/2 mice (n>=5 mice/group). Data are expressed as mean ± standard error of the mean. Statistics: unpaired t-test (*$p < 0.05$; **$p < 0.01$).

Data availability

Data will be made available on request.

Acknoledgements

This paper was supported by a grant from the Italian Ministry of Health entitled "Innovative therapeutic strategy targeting neurons with cholesterol in Huntington disease: from preclinical studies to clinical trial readiness" (RF-2016- 02361928).

Supplementary materials

Supplementary material associated with this article can be found, in the online version, at doi:10.1016/j.talo.2023.100278.

References

[1] A.F. Hofmann, L.R. Hagey, Key discoveries in bile acid chemistry and biology and their clinical applications: history of the last eight decades, J. Lipid Res. 55 (2014) 1553–1595, https://doi.org/10.1194/jlr.R049437.
[2] J.M. Dietschy, S.D. Turley, Thematic review series: brain Lipids. Cholesterol metabolism in the central nervous system during early development and in the mature animal, J. Lipid Res. 45 (2004) 1375–1397, https://doi.org/10.1194/jlr.R400004-JLR200.
[3] M. Valenza, G. Birolini, E. Cattaneo, The translational potential of cholesterol-based therapies for neurological disease, Nat. Rev. Neurol. (2023), https://doi.org/10.1038/s41582-023-00864-5.

[4] D. Lingwood, K. Simons, Lipid rafts as a membrane-organizing principle, Science 327 (2010) 46–50, https://doi.org/10.1126/science.1174621.
[5] I. Björkhem, S. Meaney, Brain cholesterol: long secret life behind a barrier, Arterioscler. Thromb. Vasc. Biol. 24 (2004) 806–815, https://doi.org/10.1161/01.ATV.0000120374.59826.1b.
[6] I. Bohanna, N. Georgiou-Karistianis, A.J. Hannan, G.F. Egan, Magnetic resonance imaging as an approach towards identifying neuropathological biomarkers for Huntington's disease, Brain Res. Rev. 58 (2008) 209–225, https://doi.org/10.1016/j.brainresrev.2008.04.001.
[7] H.D. Rosas, D.H. Salat, S.Y. Lee, A.K. Zaleta, V. Pappu, B. Fischl, D. Greve, N. Hevelone, S.M. Hersch, Cerebral cortex and the clinical expression of Huntington's disease: complexity and heterogeneity, Brain 131 (2008) 1057–1068, https://doi.org/10.1093/brain/awn025.
[8] H.J. Waldvogel, E.H. Kim, L.J. Tippett, J.-P.G. Vonsattel, R.L.M. Faull, The neuropathology of Huntington's disease, Curr. Top. Behav. Neurosci. 22 (2015) 33–80, https://doi.org/10.1007/7854_2014_354.
[9] M. Valenza, J.B. Carroll, V. Leoni, L.N. Bertram, I. Björkhem, R.R. Singaraja, S. Di Donato, D. Lutjohann, M.R. Hayden, E. Cattaneo, Cholesterol biosynthesis pathway is disturbed in YAC128 mice and is modulated by huntingtin mutation, Hum. Mol. Genet. 16 (2007) 2187–2198, https://doi.org/10.1093/hmg/ddm170.
[10] M. Valenza, V. Leoni, J.M. Karasinska, L. Petricca, J. Fan, J. Carroll, M.A. Pouladi, E. Fossale, H.P. Nguyen, O. Riess, M. MacDonald, C. Wellington, S. DiDonato, M. Hayden, E. Cattaneo, Cholesterol defect is marked across multiple rodent models of Huntington's disease and is manifest in astrocytes, J. Neurosci. 30 (2010) 10844–10850, https://doi.org/10.1523/JNEUROSCI.0917-10.2010.
[11] G. Birolini, M. Valenza, I. Ottonelli, A. Passoni, M. Favagrossa, J.T. Duskey, M. Bombaci, M.A. Vandelli, L. Colombo, R. Bagnati, C. Caccia, V. Leoni, F. Taroni, F. Forni, B. Ruozi, M. Salmona, G. Tosi, E. Cattaneo, Insights into kinetics, release, and behavioral effects of brain-targeted hybrid nanoparticles for cholesterol delivery in Huntington's disease, J. Control Release 330 (2021) 587–598, https://doi.org/10.1016/j.jconrel.2020.12.051.
[12] V. Leoni, C. Mariotti, S.J. Tabrizi, M. Valenza, E.J. Wild, S.M.D. Henley, N. Z. Hobbs, M.L. Mandelli, M. Grisoli, I. Björkhem, E. Cattaneo, S. Di Donato, Plasma 24S-hydroxycholesterol and caudate MRI in pre-manifest and early Huntington's disease, Brain 131 (2008) 2851–2859, https://doi.org/10.1093/brain/awn212.
[13] V. Leoni, J.D. Long, J.A. Mills, S. Di Donato, J.S. Paulsen, Plasma 24S-hydroxycholesterol correlation with markers of Huntington disease progression, Neurobiol. Dis. 55 (2013) 37–43, https://doi.org/10.1016/j.nbd.2013.03.013.
[14] W.J. Griffiths, P.J. Crick, Y. Wang, Methods for oxysterol analysis: past, present and future, Biochem. Pharmacol. 86 (2013) 3–14, https://doi.org/10.1016/j.bcp.2013.01.027.
[15] S. Dzeletovic, A. Babiker, E. Lund, U. Diczfalusy, Time course of oxysterol formation during in vitro oxidation of low density lipoprotein, Chem. Phys. Lipids. 78 (1995) 119–128, https://doi.org/10.1016/0009-3084(95)02489-6.
[16] M. Valenza, J.Y. Chen, E. Di Paolo, B. Ruozi, D. Belletti, C. Ferrari Bardile, V. Leoni, C. Caccia, E. Brilli, S. Di Donato, M.M. Boido, A. Vercelli, M.A. Vandelli, F. Forni, C. Cepeda, M.S. Levine, G. Tosi, E. Cattaneo, Cholesterol-loaded nanoparticles ameliorate synaptic and cognitive function in Huntington's disease mice, EMBO Mol. Med. 7 (2015) 1547–1564, https://doi.org/10.15252/emmm.201505413.
[17] J.G. Swales, G. Hamm, M.R. Clench, R.J.A. Goodwin, Mass spectrometry imaging and its application in pharmaceutical research and development: a concise review, Int. J. Mass Spectrom. 437 (2019) 99–112, https://doi.org/10.1016/j.ijms.2018.02.007.
[18] J.G. McDonald, B.M. Thompson, E.C. McCrum, D.W. Russell, Extraction and analysis of sterols in biological matrices by high performance liquid chromatography electrospray ionization mass spectrometry, Meth. Enzymol. 432 (2007) 145–170, https://doi.org/10.1016/S0076-6879(07)32006-5.
[19] W.J. Griffiths, J. Abdel-Khalik, T. Hearn, E. Yutuc, A.H. Morgan, Y. Wang, Current trends in oxysterol research, Biochem. Soc. Trans. 44 (2016) 652–658, https://doi.org/10.1042/BST20150255.
[20] L. Mangiarini, K. Sathasivam, M. Seller, B. Cozens, A. Harper, C. Hetherington, M. Lawton, Y. Trottier, H. Lehrach, S.W. Davies, G.P. Bates, Exon 1 of the HD gene with an expanded CAG repeat is sufficient to cause a progressive neurological phenotype in transgenic mice, Cell 87 (1996) 493–506, https://doi.org/10.1016/s0092-8674(00)81369-0.
[21] C. Villani, G. Sacchetti, R. Bagnati, A. Passoni, F. Fusco, M. Carli, R.W. Invernizzi, Lovastatin fails to improve motor performance and survival in methyl-CpG-binding protein2-null mice, Elife 5 (2016), https://doi.org/10.7554/eLife.22409.
[22] J.G. McDonald, D.D. Smith, A.R. Stiles, D.W. Russell, A comprehensive method for extraction and quantitative analysis of sterols and secosteroids from human plasma, J. Lipid Res. 53 (2012) 1399–1409, https://doi.org/10.1194/jlr.D022285.
[23] F. Kreilaus, A.S. Spiro, C.A. McLean, B. Garner, A.M. Jenner, Evidence for altered cholesterol metabolism in Huntington's disease post mortem brain tissue, Neuropathol. Appl. Neurobiol. 42 (2016) 535–546, https://doi.org/10.1111/nan.12286.
[24] Y. Xu, Y. Yuan, L. Smith, R. Edom, N. Weng, R. Mamidi, J. Silva, D.C. Evans, H. K. Lim, LC-ESI-MS/MS quantification of 4β-hydroxycholesterol and cholesterol in plasma samples of limited volume, J. Pharm. Biomed. Anal. 85 (2013) 145–154, https://doi.org/10.1016/j.jpba.2013.07.016.
[25] M.Q. Huang, W. Lin, W. Wang, W. Zhang, Z.J. Lin, N. Weng, Quantitation of P450 3A4 endogenous biomarker - 4β-hydroxycholesterol - in human plasma using LC/ESI-MS/MS, Biomed. Chromatogr. 28 (2014) 794–801, https://doi.org/10.1002/bmc.3131.
[26] D. Lütjohann, O. Breuer, G. Ahlborg, I. Nennesmo, A. Sidén, U. Diczfalusy, I. Björkhem, Cholesterol homeostasis in human brain: evidence for an age-dependent flux of 24S-hydroxycholesterol from the brain into the circulation, Proc. Natl. Acad. Sci. USA 93 (1996) 9799–9804, https://doi.org/10.1073/pnas.93.18.9799.